Author Manuscript

Author Manuscript

Author Manuscript

Author Manuscript

HHS Public Access

Author manuscript

Magn Reson Med. Author manuscript; available in PMC 2015 May 11.

Published in final edited form as:

Magn Reson Med. 2009 August ; 62(2): 357–364. doi:10.1002/mrm.22020.

Comparison of ^{1}H BOLD and ^{19}F MRI to investigate tumor oxygenation

Dawen Zhao, **Lan Jiang**, **Eric W. Hahn**, and **Ralph P. Mason**

Department of Radiology, University of Texas Southwestern Medical Center, Dallas, TX, USA

Abstract

^{19}F MRI oximetry and ^{1}H blood oxygen level dependent (BOLD) MRI were used to investigate tumor oxygenation in rat breast 13762NF carcinomas and correlations between the techniques were examined. A range of tissue pO_2 values was found in the nine tumors while the anesthetized rats breathed air with individual tumor pO_2 ranging from a mean of 1 to 36 torr and hypoxic fraction HF_{10} (<10 torr) ranging from 0 to 75% indicating a large intra- and inter-tumor heterogeneity. Breathing oxygen produced significant increase in tumor pO_2 (mean ΔpO_2 =50 torr) and decrease in HF_{10} ($p<0.01$). ^{1}H BOLD MRI observed using a spin echo planar imaging (EPI) sequence revealed a heterogeneous response and significant increase in mean tumor signal intensity (ΔSI =7%, $p<0.01$). R_2* measured by multi-gradient echo (MGRE) MRI decreased significantly in response to oxygen (mean $\Delta R_2^* = -4\ s^{-1}$; $p<0.05$). A significant correlation was found between changes in mean tumor pO_2 and mean EPI BOLD ΔSI accompanying oxygen breathing ($r^2 > 0.7$, $p<0.001$). Our results suggest that BOLD MRI provides information about tumor oxygenation and may be useful to predict pO_2 changes accompanying interventions. Significantly, the magnitude of the BOLD response appears to be predictive for residual tumor hypoxic fractions.

Keywords

tumor oxygenation; BOLD; ^{19}F MRI; transverse relaxation rate R_2*; oxygen; hexafluorobenzene

Introduction

Tumor oxygenation has been widely recognized as a potent factor influencing tumor response to various therapies, especially radiotherapy and hypoxia appears to promote tumor malignant progression and metastasis (1). Given the importance of tumor oxygenation, many measurement techniques have been developed (1,2). While each method has specific attributes, many are highly invasive or cannot be applied to longitudinal studies of oxygen dynamics.

BOLD (blood oxygen level dependent) MRI, extensively used in studying brain function, is increasingly being applied to assess blood oxygenation and vascular function in tumors non-

Address correspondence to: Ralph P. Mason, Ph.D., Department of Radiology, UT Southwestern Medical Center, 5323 Harry Hines Blvd., Dallas, TX 75390-9058, Tel: (214) 648-8926; Fax: (214) 648-2991, Ralph.Mason@UTSouthwestern.edu.

Author Manuscript Author Manuscript Author Manuscript Author Manuscript

invasively (3–12). The underlying rationale is that the paramagnetic deoxyhemoglobin creates microscopic field gradients, which enhance the transverse relaxation rate, R_2*, of water protons in blood and in the tissue adjacent to blood vessels. Decrease in deoxyhemoglobin concentration leads to a decreased R_2*, and thus, to an increased signal intensity in T_2*-weighted MRI (13,14). Gradient-recalled echo (GRE) or spin echo planar imaging (EPI) is sensitive to changes in R_2*. However, BOLD contrast is also influenced by other factors such as blood flow, blood volume and vascular architecture (3,15). Several recent studies have attempted to correlate BOLD MRI with tissue pO_2 measured by various techniques, notably, oxygen electrodes, oxygen sensitive fiber optic probes, ESR and ^{19}F MRI (4,11,16,17). Some of these studies have indicated a strong quantitative correlation with tissue pO_2 (11), some found a qualitative relationship (16,17), while others suggested a lack of direct correlation, yet consistent temporal trends (4).

We have developed a method for measuring tumor oxygenation and dynamics based on ^{19}F NMR EPI following direct intratumoral injection of the reporter molecule hexafluorobenzene (HFB): FREDOM (Fluorocarbon Relaxometry using Echo planar imaging for Dynamic Oxygen Mapping) (2). This technique provides quantitative pO_2 measurements at multiple specific locations simultaneously within a tumor, and reveals acute dynamic changes at individual locations with respect to interventions, such as hyperoxic gas breathing and vascular modifiers. The aim of this study was to compare ^{19}F oximetry (FREDOM) with ^{1}H BOLD MRI in evaluating tumor oxygenation in response to hyperoxic gas (100% oxygen) challenge.

Materials and Methods

Tumor Model

Rat mammary carcinoma 13762NF (originally obtained from the Division of Cancer Treatment, NCI) was implanted syngeneically in a skin pedicle surgically created on the foreback of Fisher 344 adult female rats (~150 g, n = 9, Harlan), as described in detail previously (18). Tumors were allowed to grow and were investigated when tumor volume was 0.2 to 2.1 cm^3 (mean volume = 1 cm^3). Investigations were approved by the Institutional Animal Care and Use Committee.

MRI experiments

MRI was performed using a 4.7 T horizontal bore magnet with a Varian Unity Inova system. Each rat was given ketamine hydrochloride (120 μl; 100 mg/ml, Aveco, Fort Dodge, IA) as a relaxant (i.p.) and maintained under general anesthesia (air and 1% isoflurane (Baxter International Inc., Deerfield, IL)). The oxygen reporter molecule hexafluorobenzene (HFB, 50 μl, Lancaster, Gainesville, FL) was injected directly into the tumor along two or three tracks in a single central plane of the tumor, coronal to the rat's body using a Hamilton syringe (Reno, NV) with a custom-made fine sharp needle (32G), as described in detail previously (2). A tunable ($^{1}H/^{19}F$) volume RF coil was placed around the tumor-bearing pedicle. Each animal was placed on its side in the magnet with no change in position during the whole study. A thermal blanket was used to maintain body temperature. A single 2 mm slice coronal to the rat body containing the strongest fluorine signal was chosen for both ^{19}F

Author Manuscript Author Manuscript Author Manuscript Author Manuscript

pO_2 and ^1H BOLD studies. ^1H and ^{19}F MR images were acquired using a spin-echo sequence. Overlaying the ^{19}F MR image on the corresponding ^1H image revealed the distribution of HFB.

^1H BOLD

Echo-planar imaging BOLD—A spin echo planar imaging sequence with pulse burst saturation recovery (PBSR) signal preparation was applied, as described previously (8). The initial saturation was designed to minimize in-flow effects. A series of 55 images including 5 baseline with air breathing (images 1–5) and 50 with oxygen breathing (images 6–55) was acquired on the 2 mm coronal section at 5 s intervals using MR parameters: τ = 500 ms ($\equiv$ TR), TE = 53.7 ms, field of view (FOV) = 40 × 40 mm, matrix = 32 × 32.

GRE R_2*—Multi-gradient echo (MGRE) images with 8 echoes were acquired on the same 2 mm slice during air breathing (baseline) and repeated immediately after the EPI BOLD sequence (~ 5 min after start of O_2 breathing) for 8 of 9 tumors. Acquisition parameters were: repetition time (TR) =195 ms, initial echo time (TE) = 7 ms, echo spacing = 6 ms, flip angle = 45°, FOV = 40 × 40 mm, matrix = 128 × 128, 2 averages, acquisition time = 6 min 40 s.

^{19}F Tumor tissue oximetry - *FREDOM*

Following a re-equilibration period of air breathing (> 15 min), tumor oxygenation was estimated on the basis of ^{19}F pulse burst saturation recovery (PBSR) EPI relaxometry of the HFB, as described previously (2). This approach provided pO_2 maps with 1.25 mm in plane resolution and ~3 μl voxel size (FOV = 40 × 40 mm, matrix = 32 × 32, 2 mm thick) in 6.5 minutes. The spin-lattice relaxation rate [R_1 (s^{-1}) = $1/T_1$] was estimated on a voxel-by-voxel basis using a three-parameter monoexponential function, and pO_2 was estimated using the relationship pO_2 (torr) = (R_1 – 0.0835)/0.001876 (2). Seven consecutive pO_2 measurements including two baseline and five oxygen breathing were acquired on the same 2 mm section as used for ^1H BOLD studies.

Data Analysis

Data were processed using IDL 5.3/5.4 (Research Systems, Boulder, CO). Signal intensity (SI) in the EPI BOLD study was assessed on a voxel-by-voxel basis and averaged at every time point for the whole tumor section. The signal intensity change (ΔSI) of each tumor was normalized to the mean baseline value expressed as a percentage change using the equation:

$$(\Delta SI)=(SI_M - SI_b)/SI_b \cdot 100\%,$$

where SI_M and SI_b refer to maximum mean SI and mean baseline SI, respectively.

R_2* maps were generated using all eight images with variable echo time by fitting an exponential model on a voxel-by-voxel basis. Mean R_2* of the whole section was determined for baseline air and oxygen intervention. ΔR_2* maps were obtained by subtracting R_2* oxygen map - R_2* baseline map.

Author Manuscript Author Manuscript Author Manuscript Author Manuscript

For the *FREDOM* data, typically 40–100 voxels provided an R_1 fit, and potential pO_2 value. Since noise may give an apparent relaxation curve (R_1) fit, data were selected by applying thresholds of T_1 error < 2.5 s and ratio T_{1error}/T_1 < 50%. The two criteria are used since T_1 can have a very large range from 1.5 to 12 s and thus the absolute error is particularly important for long T_1s and the ratio for short T_1s. While these criteria appear quite lax, only those voxels, which provided consistently reliable data throughout the whole time course of seven measurements, were included for further analysis.

Statistical significance was assessed using an Analysis of Variance (ANOVA) on the basis of Fisher's Protected Least Significant Difference (PLSD; Statview, SAS Inst. Inc., Cary, NC) or paired Student's t-tests. ANOVA was applied for comparison of multiple repeat measurements and the PLSD examines the importance of individual measurements on the overall population. The assumption is that inhaled gas at various time points is the independent variable, while pO_2, R_2* and BOLD signal changes are dependant variables. Paired Student t-tests were used to compare individual pairs of data such as pO_2 in a specific tumor during air or oxygen breathing.

Results

Overlay of ^{19}F on the corresponding ^{1}H MR image confirmed that HFB was distributed in both peripheral and central regions of a 2 mm thick section, located in the central plane of a representative tumor (Figure 1). The following EPI BOLD, GRE R_2* and ^{19}F oximetry measurements all interrogated this thin slice.

^{1}H BOLD

Echo-planar imaging—Normalized SI maps at different time points after switching to oxygen breathing showed heterogeneous response (Figure 2). Significant mean signal enhancement during oxygen inhalation was observed in all nine tumors with a mean ΔSI = 6.7 ± 1.4% (range from 1% to 12%; Table 1). However, individual voxel data showed some regions with negative response (Figure 2). The percentage of voxels with negative response ranged from 12% to 38% in the nine tumors. Baseline signal was quite stable, but there was a rapid response within about 25 s of switching the inhaled gas to oxygen. Some tumors showed a continual increase, which was usually biphasic and approached a stable plateau after about 3 mins. In other cases there was a transient maximum followed by a stable lower value, just marginally above baseline.

GRE R_2*—Baseline maps revealed distinct heterogeneity with R_2* ranging from 6 to 450 s^{-1} (T_2*: 2 – 166 ms, Figure 3). In response to oxygen challenge, a small, but significant decrease in R_2* was seen predominately in the tumor periphery ($p < 0.001$; Figure 3). There was no correlation between baseline R_2* and ΔR_2* on a voxel-by-voxel basis ($r^2 = 0.1$; Figure 3B). For the group of eight tumors, a significant decrease in mean R_2* (suggesting increased oxyhemoglobin level) was found (mean $\Delta R_2^* = -4 \pm 2$, $p < 0.05$, Table 1). One tumor (no. 5; Table 1) showed contrary behavior with increased mean R_2* with oxygen breathing. A very close correlation was observed between the mean R_2* values during air versus oxygen breathing (Figure 3C). A general trend was observed when the mean BOLD response for individual tumors was compared with ΔR_2* (Figure 3D). In essence large ΔR_2*

Author Manuscript Author Manuscript Author Manuscript Author Manuscript

was associated with large ΔSI, and an increase in R_2* coincided with a small signal change. However, most tumors showed a ΔR_2* of −4 ms and this was associated with a large range in BOLD signal change.

^{19}F Tumor tissue oximetry – FREDOM

pO_2 maps showed a range of baseline pO_2 values and a heterogeneous response to oxygen breathing (Figure 4, Table 1). Oxygenation appeared clustered with higher pO_2 regions appearing close to the periphery when overlaid on the anatomical ^{1}H MR images of the corresponding tumor slices. Time course of pO_2 dynamics showed differential response in both rate and magnitude (Figure 4B). For the group of 9 tumors, baseline pO_2 varied from essentially hypoxic (0.3 torr) to well oxygenated (36 torr; Table 1). With respect to oxygen challenge, mean pO_2 increased significantly in all the tumors (ΔpO_2 = 50 torr; Table 1) and hypoxic fractions (< 10 torr) decreased significantly, from a mean tumor baseline 31% to 8% ($p<0.05$). In most tumors (7 of 9) the HF_{10} was essentially eliminated (<5% residual), but in two tumors a substantial hypoxic fraction remained albeit considerably diminished compared with baseline. Histograms for the pooled individual voxels (n= 265) from the nine tumors in response to oxygen challenge revealed significant increase in pO_2 to a mean (75 ± 4 torr) and median (63 torr) ($p < 0.001$) (Figure 5A, B). Hypoxic fractions HF_5 (<5 torr) and HF_{10} (<10 torr) decreased significantly from baseline values of 18% and 34% to 8% and 10%, respectively ($p < 0.01$). In common with previous observations in this tumor line baseline pO_2 tended to decrease with tumor volume ($r^2>0.52$) and as a corollary HF_{10} increased with tumor volume ($r^2>0.49$) (19,20). A strong inverse correlation was found between tumor mean pO_2 and HF_{10} (Figure 5C). The change in pO_2 (ΔpO_2) tended to increase for tumors with higher baseline pO_2 ($r^2>0.4$), but the relationship was much stronger when comparing pO_2 during oxygen breathing versus baseline pO_2 ($r^2>0.6$; Figure 5D).

Correlation of pO_2 with ^{1}H BOLD

For the group of nine tumors, a significant linear correlation was found between mean ΔpO_2 and ΔSI, detected by ^{19}F oximetry and ^{1}H EPI BOLD ($r^2 > 0.7$, $p < 0.001$; Figure 6). However, there was a weak correlation between baseline pO_2 and ΔSI ($r^2 = 0.3$, data not shown). Likewise comparison of ΔR_2* with baseline pO_2, maximum pO_2 during oxygen breathing or ΔpO_2 indicated no correlations ($r^2<0.01$). Every tumor exhibiting a large BOLD response (ΔSI>3%) had a negligible residual hypoxic fraction (HF_{10}<5%) during oxygen breathing. In two of three tumors showing a small BOLD response a large HF_{10} remained (Figure 7).

Discussion

Oxygenation in 13762NF rat breast tumors was found to cover a considerable range with both intra- and inter-tumor heterogeneity, but a tendency towards lower pO_2 and greater hypoxia in larger tumors, as also reported previously by us (19,20). Likewise tumor response to modulation by hyperoxic gas breathing, which resulted in increased pO_2 and reduced residual hypoxic fraction was in line with previous observations (19–21). Here, we have undertaken consecutive ^{1}H MRI BOLD and ^{19}F MRI oximetry investigations to

Author Manuscript Author Manuscript Author Manuscript Author Manuscript

examine potential correlations. A strong correlation was found between mean BOLD signal response (ΔSI) and change in mean pO_2 (Figure 6) supporting previous observations in various tumor types reported by others (4,11,17). More significantly, a small BOLD response usually indicates a substantial residual hypoxic fraction, while a large BOLD response to breathing oxygen indicates that the tumor is well oxygenated or becomes well oxygenated (Figure 7).

Quantitative oximetry (absolute pO_2 values) has been shown to predict for local recurrence and disease free survival in several human cancers (notably, cervical and head and neck (22,23)). To date, electrodes have provided the only quantitative clinical pO_2 measurements in tumors, and electrodes are not only invasive, but the Eppendorf Histograph cannot easily show changes in pO_2 with respect to interventions. Furthermore, the Histograph is no longer commercially available. ^{19}F MRI based on perfluorocarbon reporters has been used to measure pO_2 in the human eye (24), but it remains generally restricted to pre-clinical animal studies (2) for two fundamental reasons: lack of access to clinical ^{19}F MRI capabilities and lack of FDA approval for human use of PFCs. ESR can also measure pO_2 distributions in rodent tumors (16,25,26), but while it has been used to measure oxygenation in humans based on India ink tattoos, it is also handicapped by lack of clinical instrumentation.

BOLD contrast MRI is an attractive surrogate for clinical pO_2 measurements, since endogenous hemoglobin itself serves as the reporter molecule. A few studies of human tumor BOLD have been presented (5,27–29), but further validation relative to other techniques is of the utmost importance. Fundamental reports from Thulborn (30) and Wright (31) together with applications of fMRI in the brain lay a strong foundation for vascular oxygen measurements. Several groups (3,4,6,8,10–14,16,17,26,32) have explored BOLD responses in diverse tumor types with respect to varying oxygen concentrations and carbogen. There is considerable evidence that signal changes in T_2*-weighted images reflect changes in pO_2. However, some investigations have shown a lack of direct correlation, *e.g*., Baudelet and Gallez (4) reported that a 10% change in signal could correspond to a small (< 25 torr) or large (approaching 100 torr) change in pO_2 in syngeneic FSA mouse tumors. Importantly, both represent large changes in pO_2 by radiobiological standards. Elas *et al.* (16) showed correlation between EPRI based on vascular trityl spin probe and sequential BOLD measurements in FSA tumors in mice. As with our study their two measurements were sequential rather than concomitant and they had the added complexity of coregistering images from separate modalities.

Fan *et al* (17) previously compared ^{19}F MR oximetry with BOLD response on a voxel-by-voxel basis in R3230AC rat breast tumors. In common with many experiments they infused perfluorocarbon emulsion, which progressively sequestered in the tumor tissue, while clearing from the vasculature. They reported that ^{19}F and ^{1}H measurement agreed in 65% of pixels, *viz*. when ^{19}F MR showed increased pO_2, then ^{1}H MR linewidth decreased reflecting less deoxyhemoglobin, as assessed using HiSS (High Spatial/Spectral resolution T_2* sensitive) measurements. Correlations were even stronger for subsets of pixels selected as showing no pO_2 change or a BOLD change. Overall they concluded that regions identified as hypoxic tended to show a small BOLD response to carbogen inhalation in the R3230AC rat breast tumors and ^{1}H MRI gave very few “false positives” (17). Our results are in accord

Author Manuscript Author Manuscript Author Manuscript Author Manuscript

with these previous observations. Tumors exhibiting a large BOLD response also showed a greater mean pO_2 response (Figure 6). Most significantly, tumors exhibiting a large BOLD response (here, defined as > 4%) showed essentially no residual hypoxic fraction (HF_{10}< 5%; Figure 7). We found no false positives and only one false negative. While breathing air 7 of 9 tumors had HF_{10} > 20% (Table 1). In all but two cases this fell below 5% with oxygen breathing, essentiality eliminating the hypoxic fraction. These remaining two tumors showed a particularly small BOLD effect (ΔSI <2.5%). Meanwhile six of seven responsive tumors exhibited a large BOLD effect (>4%). We do note that the 13762NF tumors show relatively low hypoxic fractions (HF_{10}) compared with many reports for tumors implanted in rodents. However, the values are closely in line with measurements reported using the Eppendorf Histograph in breast tumors in patients (33)

We should note differences between Karczmar's team's approach and ours. The use of systemically delivered PFC emulsions as reporter molecules tends to provide signal from well perfused tumor regions only. Indeed. Fan *et al.* (17) predominantly detected ^{19}F signal from the tumor periphery, as also noted by others (34). While our current approach allowed interrogation of central tumor regions, as well as periphery, it required direct injection of HFB into the tumor, which is invasive and samples limited regions only. Thus, it is particularly reassuring that the two approaches provide commensurate results.

BOLD changes reflect vascular oxygenation, whereas FREDOM measures tissue pO_2. As expected, the BOLD changes occurred much more rapidly (seconds, Figure 2) than the pO_2 changes (minutes, Figure 4). In the future it will be interesting to examine ^1H T_1-weighted tissue water response or so-called TOLD (Tissue Oxygen Level Dependant) response, as reported by Matsumoto *et al*. (35), since then both vascular and tissue changes can be assessed by ^1H MRI. Matsumoto *et al*. (35) examined response to hyperbaric oxygen breathing, but others have reported T_1 changes associated with hyperoxic gas in normal tissues (36) and tumors (3,10). The kinetic response of the mean BOLD signal was consistent with previous global near infrared observations in this tumor type (20,37). Changes in deoxyhemoglobin concentration generally followed a biphasic time course as also seen in the BOLD response (Figure 2B). This probably represents rapid arteriolar oxygenation followed by more sluggish response in the distant parts of the vascular tree. Meanwhile pO_2 response was more sluggish with continued increase over 30 mins (Figure 4B) for a responsive tumor. These observations are in line with previous observations based on oxygen sensitive fiber optic probes and polarographic electrodes in this tumor type (38).

BOLD MRI or susceptibility-weighted R_2* measurement based on the intrinsic paramagnetic properties of deoxyhemoglobin have been increasingly applied to assess tumor vasculature (7,9). An increase in BOLD SI or a decrease in R_2* may be related to decreased blood deoxyhemoglobin. However, BOLD SI change is also related to several other factors, *e.g.*, changes in tumor blood flow, volume, hematocrit and the ability of red blood cells to traverse tumor capillaries (3). Here, we applied a presaturation sequence across the whole tumor to minimize flow effects. It has been shown that BOLD MRI is probably less sensitive to changes in tumor oxygenation in regions containing very sparse vasculature, and hence, little deoxyhemoglobin (9). There may be concern that poorly vascularized tumors cannot show a measurable BOLD effect, due to lack of deoxyhemoglobin (9,14). As a

Author Manuscript Author Manuscript Author Manuscript Author Manuscript

corollary, we propose that poorly vascularized tumors will also be hypoxic. Thus, a small or absent BOLD effect will be indicative of hypoxia. Indeed, Rodrigues *et al*. (12) showed that well vascularized GH3 prolactinomas tended to have a much higher R_2* than sparsely vascularized Radiation-induced fibrosarcomas (RIF-1). GH3 tumors showed a large ΔR_2* in response to carbogen breathing, whereas the RIF-1 tumors showed essentially no change. Breathing carbogen enhanced the response of GH3 tumors to a single high dose of radiation (15 Gy), whereas there was no effect on RIF-1 tumors. Our range of R_2* values (54 – 116 s^{-1}) is commensurate with previous reports for animal tumors at 4.7 T (12). In terms of potential clinical applications the ability to stratify patients based on oxic or oxygenatable tumors versus hypoxic (and resistant to modulation) could be significant.

BOLD contrast is related to changes in local deoxyhemoglobin concentration. However, baseline R_2* reflects not only blood deoxyhemoglobin level, vascular blood flow and volume, but also local tissue architecture, *i.e.*, cell density, edema, necrosis. Thus, the baseline R_2* and change in R_2* (ΔR_2*) likely depends on tumor type. Recently, Robinson *et al.* (9) showed heterogeneous inter-tumoral R_2* among a variety of tumors, in which the GH3 prolactinoma had the highest mean R_2* = 89 s^{-1} and RIF-1 had the lowest value of 58 s^{-1}. In response to carbogen breathing, a significant decrease in R_2* (−23 s^{-1}) was found in the GH3 prolactinoma, whereas the RIF-1 fibrosarcomas showed a little increase in R_2* (1 s^{-1}). In the current study, seven out of eight tumors had a modest decrease in R_2* (mean = −4 s^{-1}), while R_2* increased in one tumor (# 5) in response to oxygen breathing. As expected, the largest ΔSI in response to oxygen breathing coincided with a large decrease in R_2* and the one tumor with increased R_2* showed small ΔSI. However, most tumors had similar ΔR_2* (about 4 s^{-1}) yet a large range of ΔSIs (Figure 3D). Generally, there was no significant correlation between baseline ΔR_2* values and R_2* (Figure 3B, Table. 1). There was a strong correlation between mean R_2* measured during air or oxygen breathing (Figure 3C).

In the past, we had used a thick section (essentially projection) for ^{19}F MR oximetry (FREDOM) studies (2). The 2 mm thick slice used here allowed more satisfactory spatial correlation between ^{19}F oximetry and ^{1}H BOLD contrast. The success of FREDOM depends largely on the signal-to-noise ratio (SNR) of the acquired images. No obvious decrease in SNR due to reduced slice thickness was seen in the current study, which we attribute to greater emphasis on injecting the HFB in a narrow plane and the ability to image oblique angles in the upgraded Varian Inova system. On average, 29 voxels (range 10 to 43) provided reliable pO_2 readings which were traceable throughout the oxygen challenge in each tumor.

We had hoped to correlate individual voxels in both ^{19}F and ^{1}H EPI (FREDOM vs. BOLD). However, the directly corresponding voxels did not allow meaningful correlation. Signal voids were observed, which had only 10 to 25% as much ^{1}H signal as surrounding tumor (Figure 1A). Overlaying ^{19}F on ^{1}H images showed that the low ^{1}H signal intensity regions corresponded with ^{19}F signal (Figure 1B). In addition the R_2* values were typically an order of magnitude smaller (14 to 37 s^{-1}, as opposed to 100 s^{-1}) with smaller and sometimes opposite changes in R_2* compared with surrounding voxels in response to breathing oxygen. We have previously observed such signal voids in ^{1}H images of tumors with HFB (19) and

Author Manuscript Author Manuscript Author Manuscript Author Manuscript

the new alternative ^{1}H MRI pO_2 reporter under development hexamethyldisiloxane (39). While ^{1}H and ^{19}F voxels did not allow direct correlation, we believe that the judicious placement of reporter molecule in central and peripheral locations can provide a representation of the whole tumor, and thus, correlation with non-labeled regions is reasonable. Importantly, pO_2 values and dynamics observed using FREDOM are highly consistent with other oximetry methods in rat breast and prostate tumors, such as electrodes (38,40), fiber optic probes (37,41) and immuno histochemistry (42).

Oxygen breathing produced a significant increase in ^{19}F measured pO_2, EPI BOLD SI and decrease in GRE R_2* on the same section of tumor. Data indicated a strong correlation between $\%\Delta SI$ and ΔpO_2 (Figure 6). Although a significant increase in global mean SI was found in all tumors by BOLD in the current study, voxel-by-voxel data analysis showed oxygen breathing induced signal loss in many voxels for each tumor, averaged as 20% of the total voxels. Similar findings have been observed in other tumor types by others and us (6,8,10,14). Indeed, Fan *et al.* (17) previously remarked that correlates between mean BOLD and pO_2 were stronger when the whole tumor was considered, as opposed to individual regions. In a slightly different context Baudelet *et al* (43) reported a better correlation between mean tumor BOLD signal response and vascular k_{ep} than for individual voxels.

The ability to identify hypoxia could have far-reaching implications for radiotherapy. We have previously shown correlations between tumor pO_2 measured by ^{19}F MRI (FREDOM) and response to single high dose irradiation in Dunning prostate R3327-HI and AT1 tumors (44,45). Furthermore, we could correctly assess the ability to alter pO_2 and modulate response to irradiation. Karczmar's team also demonstrated the ability of BOLD (*viz*. HiSS) to predict the relative efficacy of tumor oxygenating agents (46). ^{1}H MRI BOLD assessment would be far more practical in the clinic and we believe our results together with the previous report from Fan *et al*. (17) provide strong impetus for translation.

Acknowledgement

This work was supported by DOD Breast Cancer Initiative Awards IDEA DAMD 17-03-1-0363 (DZ) and pre doctoral fellowship DAMD 17-02-1-0592 (LJ), in conjunction with NCI RO1 CA79515/EB002762 and the Southwestern Small Animal Imaging research program (SW-SAIRP supported by U24 CA12660801 and P20 Pre-ICMIC CA86354). MRI experiments were performed in the Advanced Imaging Research Center (formerly, Mary Nell & Ralph B. Rogers MR Center) an NIH BTRP # P41-RR02584 facility. We are grateful to Ammar Adams and Dr. Matthew Merritt for technical and collegial support.

References

1. Tatum JL, Kelloff GJ, Gillies RJ, Arbeit JM, Brown JM, Chao KS, Chapman JD, Eckelman WC, Fyles AW, Giaccia AJ, Hill RP, Koch CJ, Krishna MC, Krohn KA, Lewis JS, Mason RP, Melillo G, Padhani AR, Powis G, Rajendran JG, Reba R, Robinson SP, Semenza GL, Swartz HM, Vaupel P, Yang D, Croft B, Hoffman J, Liu G, Stone H, Sullivan D. Hypoxia: Importance in tumor biology, noninvasive measurement by imaging, and value of its measurement in the management of cancer therapy. Int J Radiat Biol. 2006; 82(10):699–757. [PubMed: 17118889]
2. Zhao D, Jiang L, Mason RP. Measuring Changes in Tumor Oxygenation. Methods Enzymol. 2004; 386:378–418. [PubMed: 15120262]
3. Howe FA, Robinson SP, Rodrigues LM, Griffiths JR. Flow and oxygenation dependent (FLOOD) contrast MR imaging to monitor the response of rat tumors to carbogen breathing. Magn Reson Imaging. 1999; 17:1307–1318. [PubMed: 10576716]

Author Manuscript Author Manuscript Author Manuscript Author Manuscript

4. Baudelet C, Gallez B. How does blood oxygen level-dependent (BOLD) contrast correlate with oxygen partial pressure (pO_2) inside tumors? Magn Reson Med. 2002; 48:980–986. [PubMed: 12465107]
5. Padhani A, Krohn K, Lewis J, Alber M. Imaging oxygenation of human tumours. Europ Radiol. 2007; 17(4):861–872.
6. Thomas CD, Chenu E, Walczak C, Plessis MJ, Perin F, Volk A. Morphological and carbogen-based functional MRI of a chemically induced liver tumor model in mice. Magn Reson Med. 2003; 50:522–530. [PubMed: 12939760]
7. Neeman M, Dafni H, Bukhari O, Braun RD, Dewhirst MW. In vivo BOLD contrast MRI mapping of subcutaneous vascular function and maturation: validation by intravital microscopy. Magn Reson Med. 2001; 45:887–898. [PubMed: 11323816]
8. Jiang L, Zhao D, Constantinescu A, Mason RP. Comparison of BOLD contrast and Gd-DTPA Dynamic Contrast Enhanced imaging in rat prostate tumor. Magn Reson Med. 2004; 51:953–960. [PubMed: 15122677]
9. Robinson SP, Rijken PF, Howe FA, McSheehy PM, van der Sanden BP, Heerschap A, Stubbs M, Van Der Kogel AJ, Griffiths JR. Tumor vascular architecture and function evaluated by non-invasive susceptibility MRI methods and immunohistochemistry. J Magn Reson Imaging. 2003; 17:445–454. [PubMed: 12655584]
10. Peller M, Weissfloch L, Stehling MK, Weber J, Bruening R, Senekowitsch-Schmidtke R, Molls M, Reiser M. Oxygen-induced MR signal changes in murine tumors. Magn Reson Imaging. 1998; 16:799–809. [PubMed: 9811145]
11. Al-Hallaq HA, River JN, Zamora M, Oikawa H, Karczmar GS. Correlation of magnetic resonance and oxygen microelectrode measurements of carbogen-induced changes in tumor oxygenation. Int J Radiat Oncol Biol Phys. 1998; 41(1):151–159. [PubMed: 9588930]
12. Rodrigues LM, Howe FA, Griffiths JR, Robinson SP. Tumor R-2 * is a prognostic indicator of acute radiotherapeutic response in rodent tumors. Journal of Magnetic Resonance Imaging. 2004; 19(4):482–488. [PubMed: 15065173]
13. Robinson SP, Howe FA, Rodrigues LM, Stubbs M, Griffiths JR. Magnetic resonance imaging techniques for monitoring changes in tumor oxygenation and blood flow. Semin Radiat Oncol. 1998; 8(3):198–207.
14. Baudelet C, Gallez B. Current issues in the utility of blood oxygen level dependent MRI for the assessment of modulations in tumor oxygenation. Curr Med Imaging Rev. 2005; 1:229–243.
15. Duyn JH, Moonen CT, van Yperen GH, de Boer RW, Luyten PR. Inflow versus deoxyhemoglobin effects in BOLD functional MRI using gradient echoes at 1.5 T. NMR Biomed. 1994; 7(1–2):83–88. [PubMed: 8068530]
16. Elas M, Williams BB, Parasca A, Mailer C, Pelizzari CA, Lewis MA, River JN, Karczmar GS, Barth ED, Halpern HJ. Quantitative tumor oxymetric images from 4D electron paramagnetic resonance imaging (EPRI): Methodology and comparison with blood oxygen level-dependent (BOLD) MRI. Magn Reson Med. 2003; 49:682–691. [PubMed: 12652539]
17. Fan X, River JN, Zamora M, Al-Hallaq HA, Karczmar GS. Effect of carbogen on tumor oxygenation: combined fluorine-19 and proton MRI measurements. Int J Radiat Oncol Biol Phys. 2002; 54:1202–1209. [PubMed: 12419449]
18. Hahn EW, Peschke P, Mason RP, Babcock EE, Antich PP. Isolated tumor growth in a surgically formed skin pedicle in the rat: A new tumor model for NMR studies. Magn Reson Imaging. 1993; 11:1007–1017. [PubMed: 8231664]
19. Song Y, Constantinescu A, Mason RP. Dynamic Breast tumor oximetry: the development of Prognostic Radiology. Technol Cancer Res Treat. 2002; 1(6):471–478. [PubMed: 12625774]
20. Xia M, Kodibagkar V, Liu H, Mason RP. Tumour oxygen dynamics measured simultaneously by near infrared spectroscopy and ^{19}F magnetic resonance imaging in rats. Phys Med Biol. 2006; 51:45–60. [PubMed: 16357430]
21. Zhao D, Jiang L, Hahn EW, Mason RP. Tumor physiological response to combretastatin A4 phosphate assessed by MRI. Int J Radiat Oncol Biol Phys. 2005; 62:872–880. [PubMed: 15936572]

Author Manuscript Author Manuscript Author Manuscript Author Manuscript

22. Fyles A, Milosevic M, Hedley D, Pintilie M, Levin W, Manchul L, Hill RP. Tumor hypoxia has independent predictor impact only in patients with node-negative cervix cancer. J Clin Oncol. 2002; 20(3):680–687. [PubMed: 11821448]
23. Brizel DM, Sibly GS, Prosmitz LR, Scher RL, Dewhirst MW. Tumor hypoxia adversely affects the prognosis of carcinoma of the head and neck. Int J Radiat Oncol Biol Phys. 1997; 38:285–289. [PubMed: 9226314]
24. Wilson C, Berkowitz B, McCuen B, Charles C. Measurement of preretinal pO_2 in the vitrectomized human eye using ^{19}F NMR. Arch Ophthalmol. 1992; 110:1098–1100. [PubMed: 1497523]
25. Bratasz A, Pandian RP, Deng Y, Petryakov S, Grecula JC, Gupta N, Kuppusamy P. In vivo imaging of changes in tumor oxygenation during growth and after treatment. Magn Reson Med. 2007; 57(5):950–959. [PubMed: 17457861]
26. Dunn JF, O'Hara JA, Zaim-Wadghiri Y, Lei H, Meyerand ME, Grinberg OY, Hou H, Hoopes PJ, Demidenko E, Swartz HM. Changes in oxygenation of intracranial tumors with carbogen: a BOLD MRI and EPR oximetry study. JMRI. 2002; 16:511–521. [PubMed: 12412027]
27. Taylor NJ, Baddeley H, Goodchild KA, Powell ME, Thoumine M, Culver LA, Stirling JJ, Saunders MI, Hoskin PJ, Phillips H, Padhani AR, Griffiths JR. BOLD MRI of human tumor oxygenation during carbogen breathing. JMRI. 2001; 14:156–163. [PubMed: 11477674]
28. Rijpkema M, Kaanders JH, Joosten FB, van der Kogel AJ, Heerschap A. Effects of breathing a hyperoxic hypercapnic gas mixture on blood oxygenation and vascularity of head-and-neck tumors as measured by magnetic resonance imaging. Int J Radiat Oncol Biol Phys. 2002; 53:1185–1191. [PubMed: 12128119]
29. Jiang, L.; McColl, R.; Weatherall, P.; Tripathy, D.; Mason, RP. ISMRM 13th Scientific Meeting. Miami Beach, Fl: 2005. BOLD and Gd-DTPA Contrast Enhanced MRI for Early Assessment of Breast Cancer Chemotherapy; p. 408
30. Thulborn KR, Waterton JC, Matthews PM, Radda GK. Oxygenation dependence of the transverse relaxation time of water protons in whole blood at high field. Biochim Biophys Acta. 1982; 714:265–270. [PubMed: 6275909]
31. Wright GA, Hu BS, Macovski A. Estimating oxygen saturation of blood in vivo with MR imaging at 1.5 T. JMRI. 1991; 1:275–283. [PubMed: 1802140]
32. Robinson SP, Collingridge DR, Howe FA, Rodrigues LM, Chaplin DJ, Griffiths JR. Tumor response to hypercapnia and hyperoxia monitored by FLOOD magnetic resonance imaging. NMR Biomed. 1999; 12:98–106. [PubMed: 10392806]
33. Vaupel P, Hockel M, Mayer A. Detection and characterization of tumor hypoxia using pO(2) histography. Antioxid Redox Signal. 2007; 9(8):1221–1235. [PubMed: 17536958]
34. Mason RP, Antich PP, Babcock EE, Constantinescu A, Peschke P, Hahn EW. Non-invasive determination of tumor oxygen tension and local variation with growth. Int J Radiat Oncol Biol Phys. 1994; 29:95–103. [PubMed: 8175452]
35. Matsumoto K, Bernardo M, Subramanian S, Choyke P, Mitchell JB, Krishna MC, Lizak MJ. MR assessment of changes of tumor in response to hyperbaric oxygen treatment. Magn Reson Med. 2006; 56(2):240–246. [PubMed: 16795082]
36. O'Connor JPB, Jackson A, Buonaccorsi GA, Buckley DL, Roberts C, Watson Y, Cheung S, McGrath DM, Naish JH, Rose CJ, Dark PM, Jayson GC, Parker GJM. Organ-specific effects of oxygen and carbogen gas inhalation on tissue longitudinal relaxation times. Magn Reson Med. 2007; 58(3):490–496. [PubMed: 17763345]
37. Gu Y, Bourke V, Kim JG, Constantinescu A, Mason RP, Liu H. Dynamic Response of Breast Tumor Oxygenation to Hyperoxic Respiratory Challenge Monitored with Three Oxygen-Sensitive Parameters. Applied Optics. 2003; 42:1–8.
38. Kim JG, Zhao D, Constantinescu A, Mason RP, Liu H. Interplay of Tumor Vascular Oxygenation and Tumor pO_2 Observed Using NIRS, Oxygen Needle Electrode, and ^{19}F MR pO_2 Mapping. J Biomed Optics. 2003; 8:53–62.
39. Kodibagkar VD, Wang X, Pacheco-Torres J, Gulaka P, Mason RP. Proton Imaging of Silanes to map Tissue Oxygenation Levels (PISTOL): a tool for quantitative tissue oximetry. NMR Biomed. 2008; 21:899–907. [PubMed: 18574806]

Author Manuscript Author Manuscript Author Manuscript Author Manuscript

40. Mason, RP.; Hunjan, S.; Constantinescu, A.; Song, Y.; Zhao, D.; Hahn, EW.; Antich, PP.; Peschke, P. Tumor oximetry: Comparison of ^{19}F MR EPI and electrodes. In: Dunn, JF.; Swartz, HM., editors. Oxygen Transport to Tissue XXIV. Volume 530, Advances in Experimental Medicine and Biology. New York: Kluwer; 2003. p. 19-28.

41. Zhao D, Constantinescu A, Hahn EW, Mason RP. Tumor oxygen dynamics with respect to growth and respiratory challenge: investigation of the Dunning prostate R3327-HI tumor. Radiat Res. 2001; 156:510–520. [PubMed: 11604064]

42. Zhao D, Ran S, Constantinescu A, Hahn EW, Mason RP. Tumor oxygen dynamics: correlation of in vivo MRI with histological findings. Neoplasia. 2003; 5(4):308–318. [PubMed: 14511402]

43. Baudelet C, Cron GO, Gallez B. Determination of the maturity and functionality of tumor vasculature by MRI: Correlation between BOLD-MRI and DCE-MRI using P792 in experimental fibrosarcoma tumors. Magnetic Resonance in Medicine. 2006; 56(5):1041–1049. [PubMed: 16986109]

44. Bourke VA, Zhao D, Gilio J, Chang C-H, Jiang L, Hahn EW, Mason RP. Correlation of Radiation Response with Tumor Oxygenation in the Dunning Prostate R3327-AT1 Tumor. Int J Radiat Oncol Biol Phys. 2007; 67(4):1179–1186. [PubMed: 17336219]

45. Zhao D, Constantinescu A, Chang C-H, Hahn EW, Mason RP. Correlation of Tumor Oxygen Dynamics with Radiation Response of the Dunning Prostate R3327-HI Tumor. Radiat Res. 2003; 159:621–631. [PubMed: 12710873]

46. Al-Hallaq HA, Zamora M, Fish BL, Farrell A, Moulder JE, Karczmar GS. MRI measurements correctly predict the relative effects of tumor oxygenating agents on hypoxic fraction in rodent BA1112 tumors. Int J Radiat Oncol Biol Phys. 2000; 47:481–488. [PubMed: 10802376]

Author Manuscript Author Manuscript Author Manuscript Author Manuscript

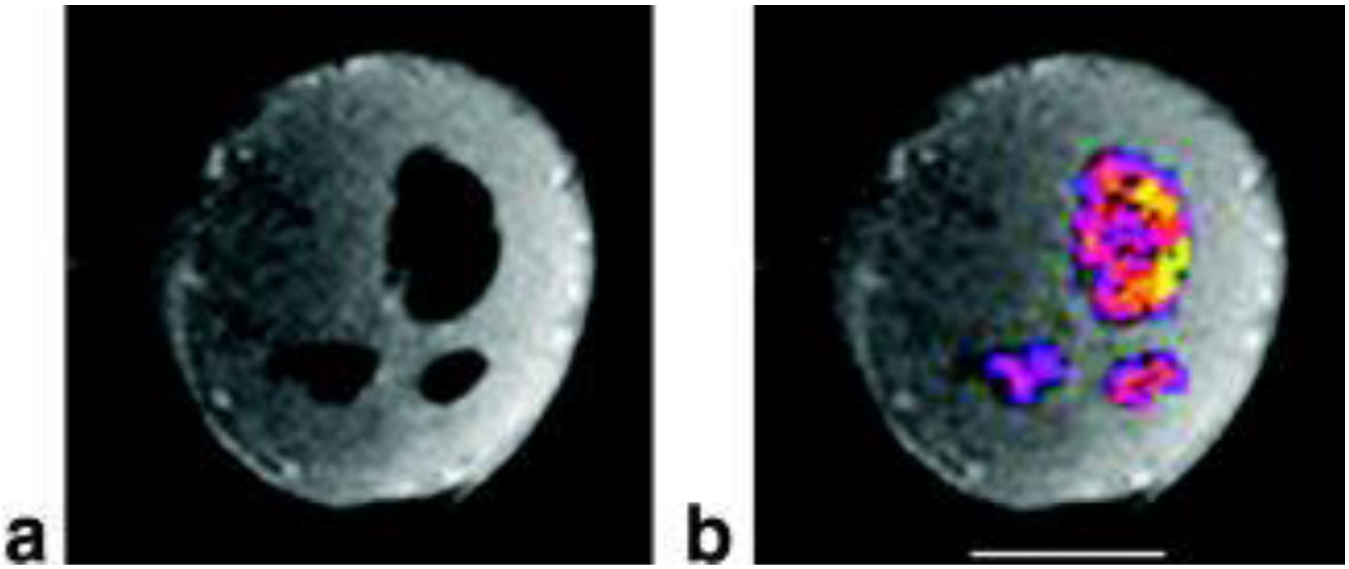

Figure 1. Distribution of oxygen reporter probe

A. ^{1}H T_1-weighted MR image of 2 mm slice through tumor showing signal voids corresponding to presence of HFB reporter molecule.

B. Overlay of ^{19}F signal intensity on ^{1}H image showing distribution of oxygen reporter probe hexafluorobenzene (HFB) in both central and peripheral tumor regions (#2 in Table 1). Bar = 0.5 cm.

Author Manuscript Author Manuscript Author Manuscript Author Manuscript

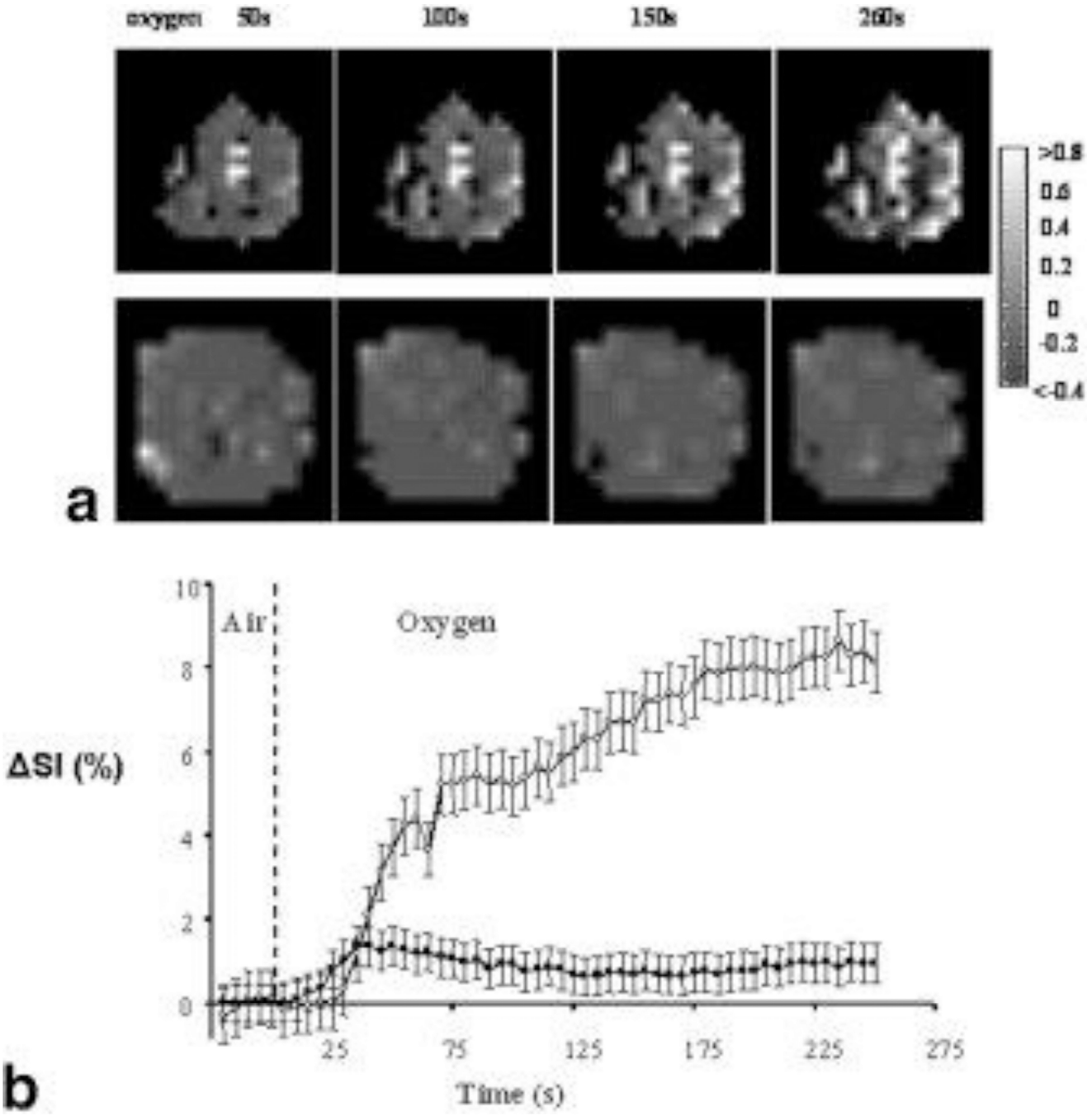

Figure 2. Variations in T_2* weighted images with oxygen challenge (BOLD)

A. Normalized spin echo planar images of two tumors acquired at several time points after switching to oxygen breathing. In response to oxygen breathing the two tumors (upper, #2 0.4 cm^3; lower, #6 1.4 cm^3) showed heterogeneous signal enhancement. Regions of decreased signal intensity were also observed (dark regions).

B. Variations of normalized signal intensity change (ΔSI) versus time for these tumors with respect to oxygen challenge. Both tumors showed an initial rapid response. For tumor #2 (○) this became biphasic reaching a plateau with 9% increase after about 200 s of oxygen

Author Manuscript Author Manuscript Author Manuscript Author Manuscript

breathing. The second tumor (#6, ■) rapidly reached a peak value of ΔSI = 1.4% after 35 s, then gradually decreased to a plateau at about 0.5% increase. Data points are mean values ± standard error.

Author Manuscript Author Manuscript Author Manuscript Author Manuscript

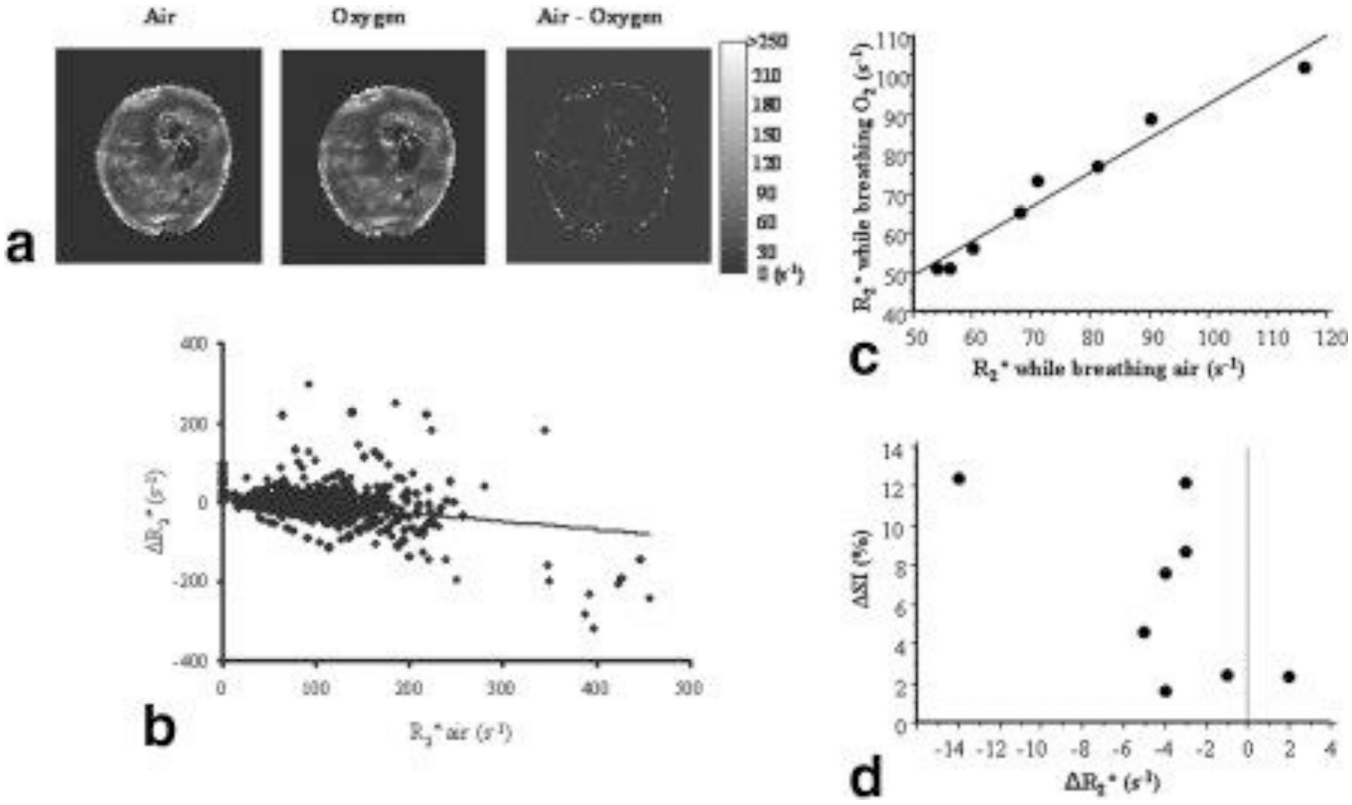

Figure 3. Response of R_2* to oxygen breathing

A. R_2* maps showed heterogeneous baseline R_2* values for tumor #2. Top left: R_2* while breathing air; Center R_2* after 5 min breathing oxygen; right difference map obtained by subtracting the oxygen map from the air map (mean $\Delta R_2^* = -2.6\ s^{-1}$).

B. A voxel-voxel comparison (n = 2056) between baseline R_2* and ΔR_2* showed a poor correlation ($r^2 = 0.1$).

C. Comparison of mean tumor R_2* measured while rat breathed oxygen versus air showed a strong correlation ($r^2 > 0.96$).

D. Comparison of mean signal change in T_2*-weighted image versus change in mean R_2* in tumors accompanying change in gas from air to oxygen breathing. No linear correlation was observed, but greater change in R_2* was accompanied by changes in signal intensity.

Author Manuscript Author Manuscript Author Manuscript Author Manuscript

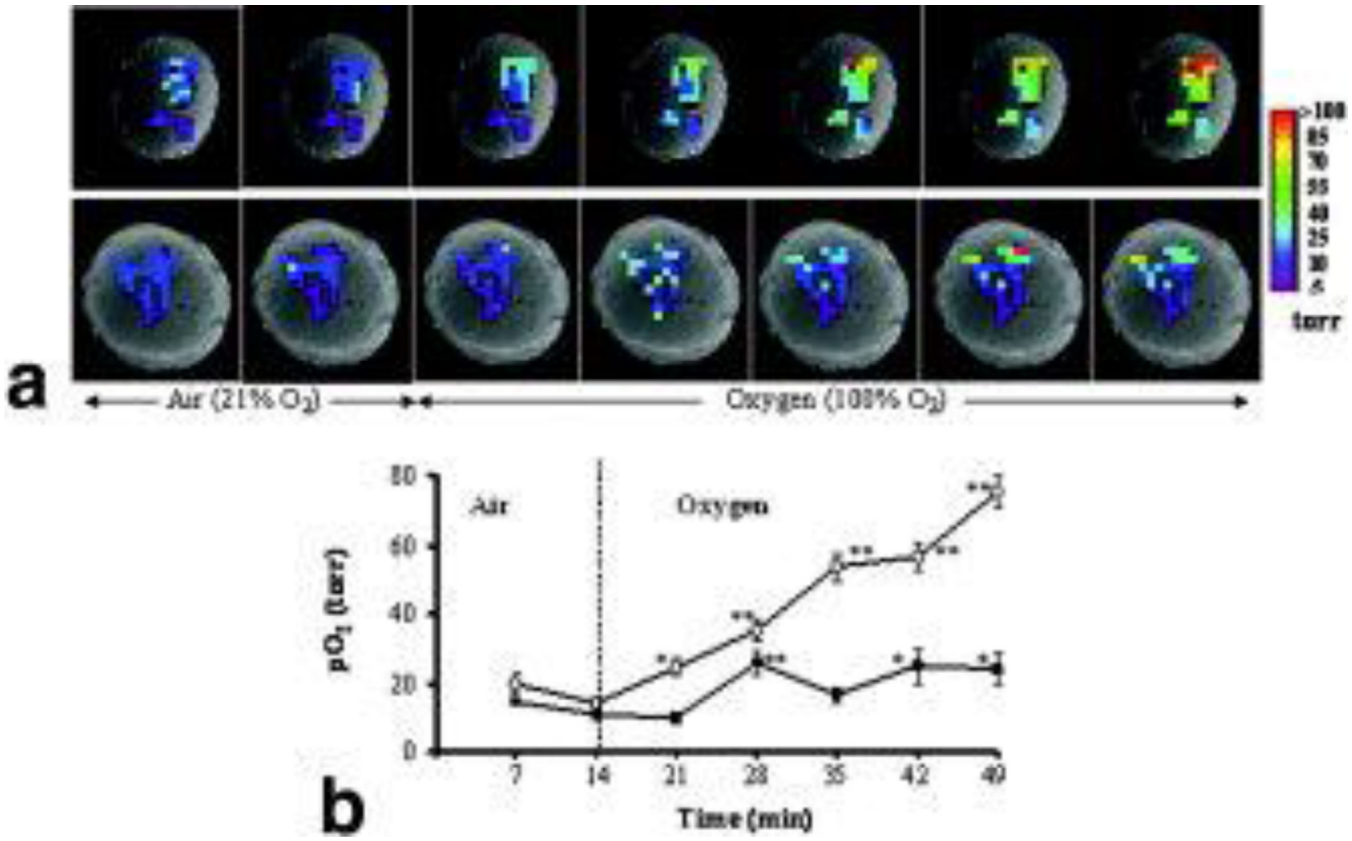

Figure 4. Variation of pO_2 with oxygen challenge

A. pO_2 maps obtained at successive times overlaid on T_1-weighted ^1H images of two tumors (#2 and #6). A range of pO_2 values was observed in both tumors under baseline conditions. In response to breathing oxygen, all the individual locations (34 voxels) in tumor # 2 (upper row) responded significantly and became well oxygenated. By contrast, some of initially hypoxic regions in tumor #6 (lower row) remained hypoxic, while others became well oxygenated.

B. Variation in mean pO_2 of each tumor. Tumor #2 (○; mean baseline = 17 torr) showed significantly increased pO_2 within 7 min of oxygen breathing, and continued to increase reaching 76 torr during the final measurement (49 min). Tumor #6 (■, mean baseline pO_2 = 13 torr) reached a peak value (26 torr) after 14 min, but the settled back to a lower level. * $p < 0.05$; ** $p < 0.001$.

Author Manuscript Author Manuscript Author Manuscript Author Manuscript

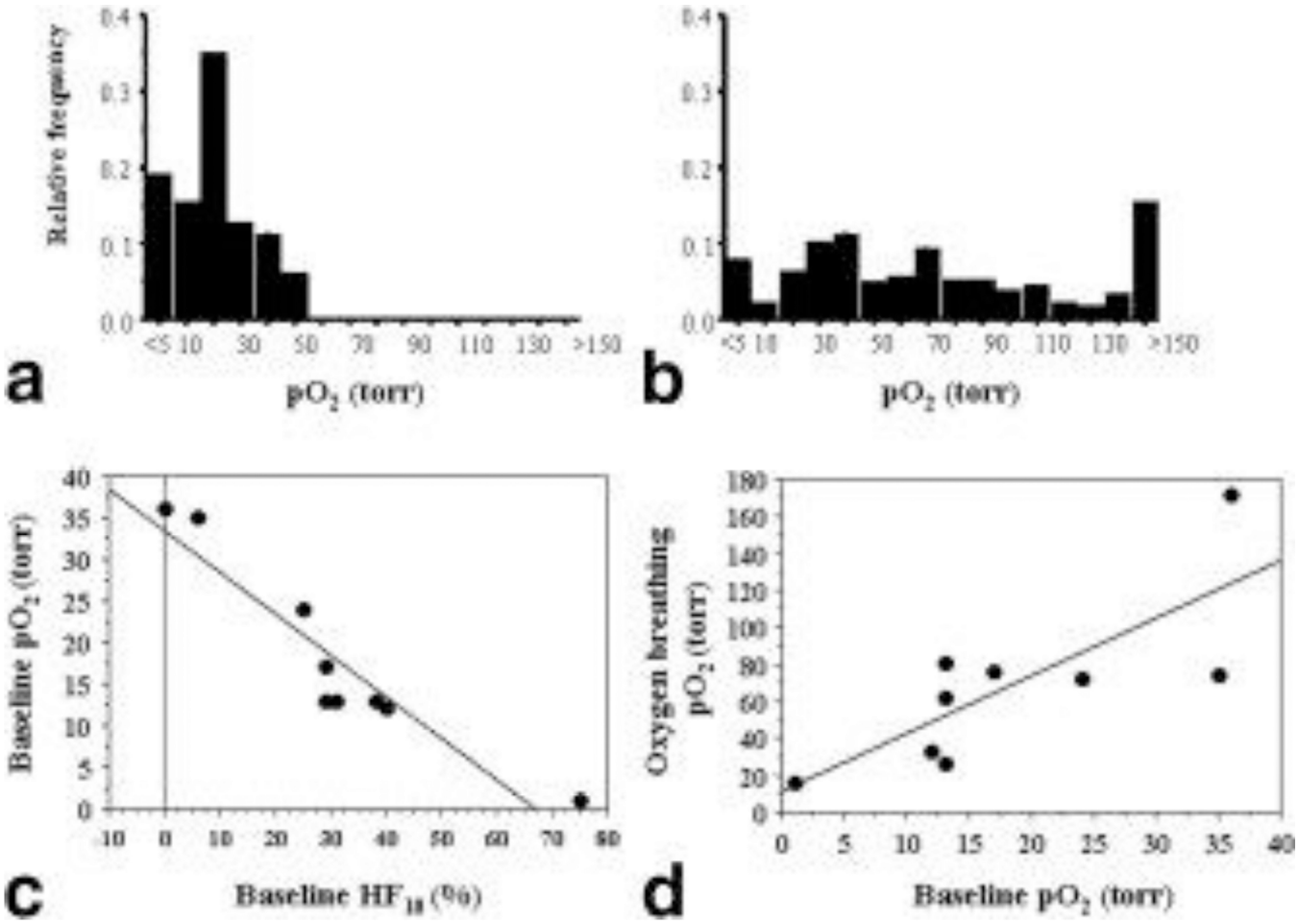

Figure 5. Tumor oxygen tension distribution

A. Pooled pO_2 values for individual regions (265) from the nine tumors showed a range of baseline pO_2 values from hypoxia (<5 torr) to 55 torr, with a mean (x) = 15 ± 1 torr and median (m) = 13.1 torr, while rats breathed air. Binning is based on ranges, *e.g.*, 10 refers to $5 \leq pO_2 < 10$ torr.

B. Oxygen breathing produced a significant increase in pO_2 with mean (75 ± 4 torr) and median (63 torr) ($p < 0.001$). Hypoxic fractions HF_5 (<5 torr) and HF_{10} (<10 torr) decreased significantly from baseline values of 18% and 34% to 8% and 10%, respectively ($p < 0.01$).

C. Correlation between mean baseline pO_2 and hypoxic fraction showed inverse relationship ($r^2 > 0.87$).

D. Dependence of pO_2 achieved with oxygen breathing on baseline pO_2 ($r^2 > 0.6$)

Author Manuscript Author Manuscript Author Manuscript Author Manuscript

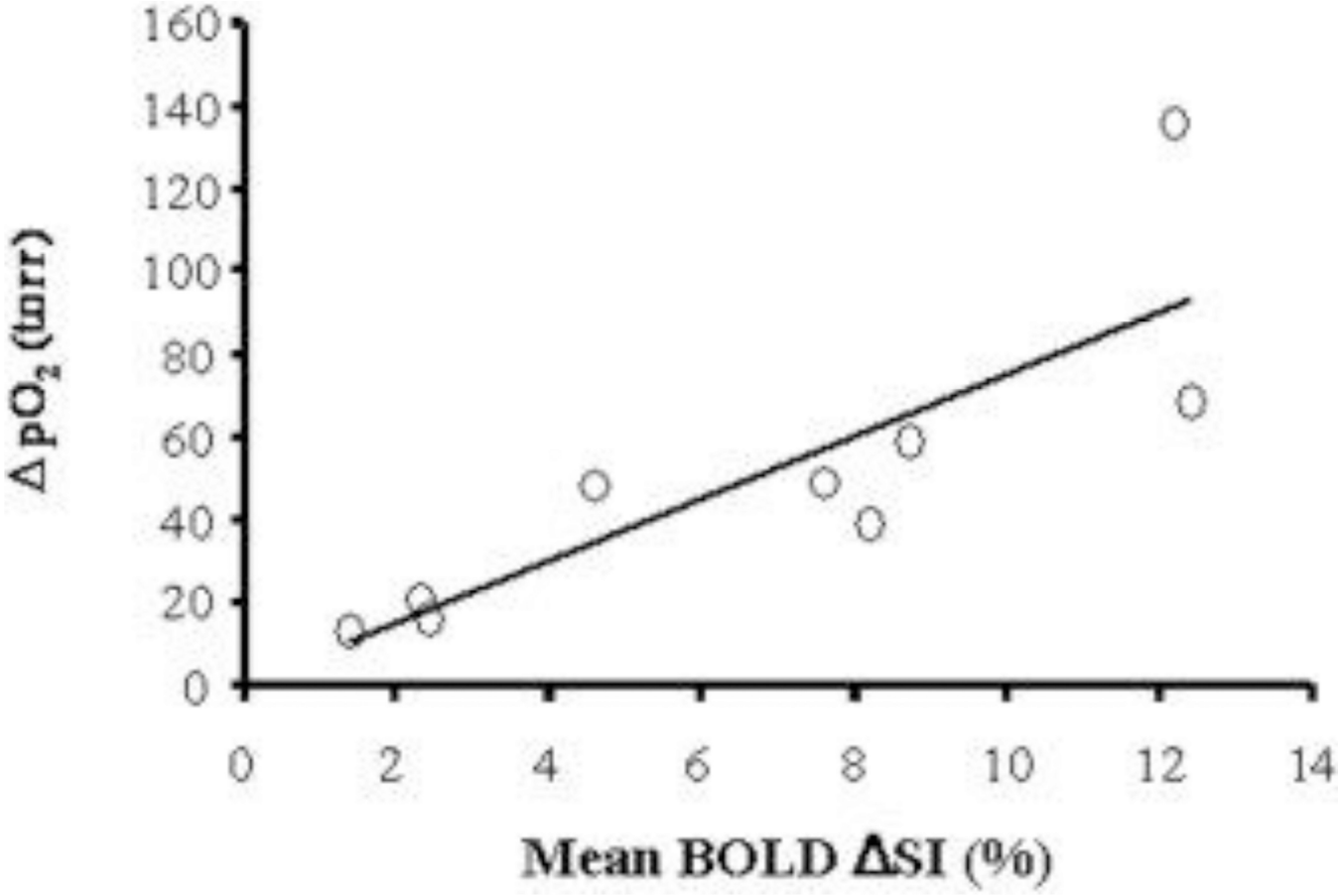

Figure 6. Correlation of pO_2 and BOLD responses to oxygen challenge

A significant linear correlation was found between mean increase in tissue pO_2 (ΔpO_2) and mean spin echo planar BOLD signal increase in the nine tumors with respect to oxygen intervention ($r^2 > 0.7$; $p < 0.001$).

Author Manuscript Author Manuscript Author Manuscript Author Manuscript

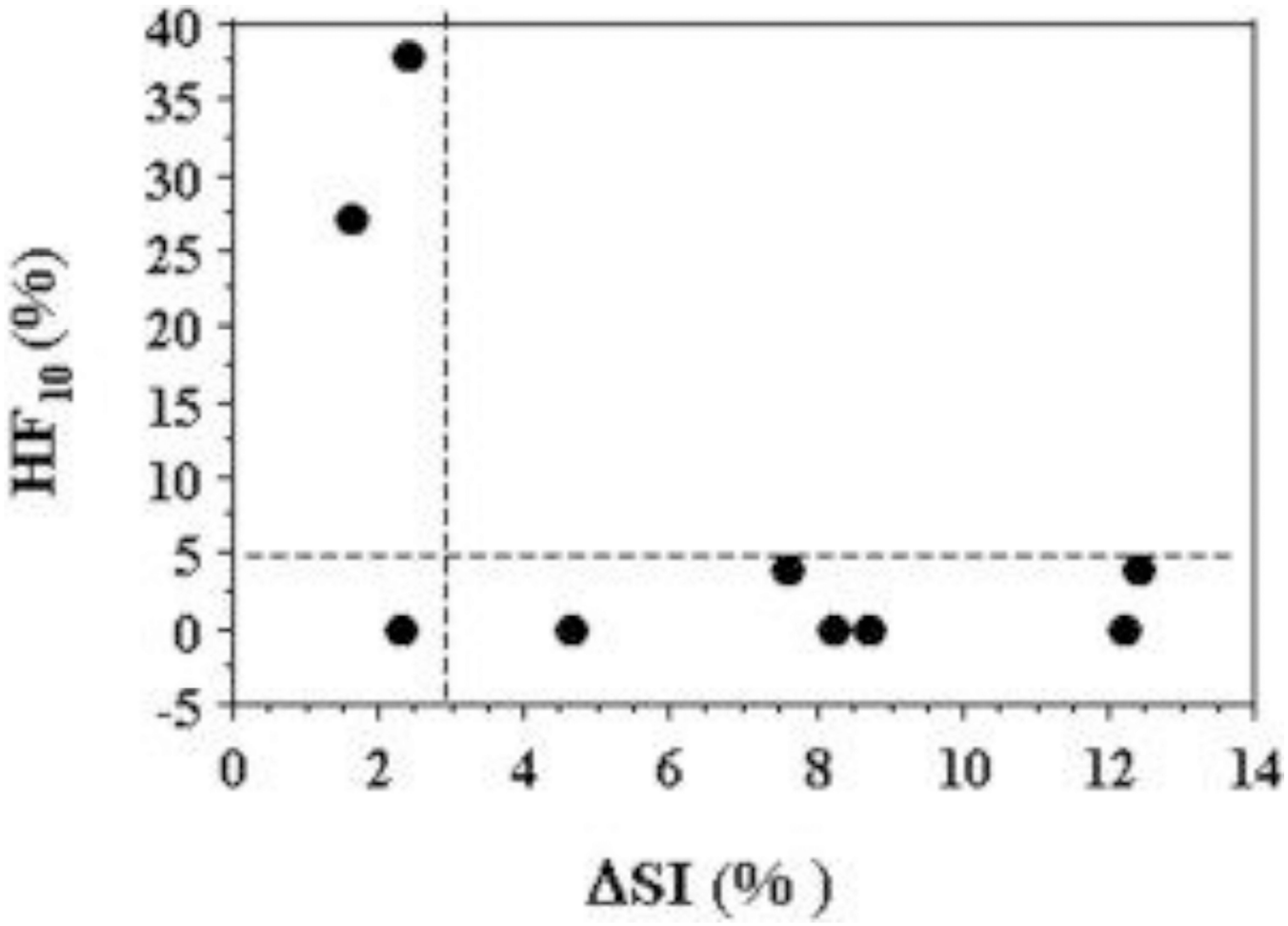

Figure 7. Assessment of residual hypoxic fraction

Comparison of the final hypoxic fraction (HF_{10}) with oxygen breathing as a function of BOLD signal response (ΔSI) suggests strong predictive value. For most tumors (6 of 9) a large BOLD response coincided with low residual HF_{10}. A small BOLD response indicated a large residual hypoxic fraction in 2 of 3 tumors.

Author Manuscript Author Manuscript Author Manuscript Author Manuscript

Magn Reson Med. Author manuscript; available in PMC 2015 May 11.

Table 1

Comparison of pO_2, BOLD and R_2* in individual tumors

Tumor #	Tumor volume (cm^3)	^{19}F oximetry					BOLD EPI (%)	R_2* (s^{-1})		
		21% O_2		100% O_2		ΔpO_2 (torr)		21% O_2	100% O_2	ΔR_2*
		pO_2 (torr)$^{\alpha}$	HF_{10} (%)	pO_2 (torr)$^{\beta}$	HF_{10} (%)					
1	0.3	36 ± 1	0	172 ± 7**	0	136	12.2 ± 0.6	54 ± 1	51 ± 1*	−3
2	0.4	17 ± 2	29	76 ± 4**	0	59	8.7 ± 0.5	68 ± 1	65 ± 1**	−3
3	0.4	13 ± 2	31	62 ± 8**	4	49	7.6 ± 0.6	81 ± 1	77 ± 1**	−4
4	0.2	13 ± 1	29	81 ± 6**	4	68	12.4 ± 0.4	116 ± 2	102 ± 2**	−14
5	2.1	12 ± 1	40	33 ± 4*	0	21	2.3 ± 0.6	71 ± 1	73 ± 1	2
6	1.4	13 ± 1	38	26 ± 5**	27	13	1.6 ± 0.5	60 ± 1	56 ± 1**	−4
7	1.0	24 ± 5	25	72 ± 12**	0	48	4.6 ± 0.8	56 ± 1	51 ± 1**	−5
8	2.1	1 ± 2	75	16 ± 9*	38	16	2.4 ± 0.6	90 ± 1	89 ± 1	−1
9	0.8	35 ± 5	6	74 ± 9**	0	39	8.2 ± 0.6	NA	NA	NA
Mean	1.0 ± 0.2	18 ± 4	31 ± 7	68 ± 15*	8 ± 4*	50 ± 13	6.7 ± 1.4	74 ± 7	70 ± 6*	−4 ± 2

NA: not measured;

* $p < 0.05$,

** $p < 0.001$ from baseline (21% O_2).

$^{\alpha}$Mean pO_2 over all voxels in the two repeated baseline measurements.

$^{\beta}$mean highest pO_2 observed in all voxels during 5 oxygen breathing measurements.